

## Characterizing Groundwater Aquifers in Warasia, Ambon City Using Electrical Resistivity Tomography Data and Archie's Law

**Samsul Bahri<sup>1,a,\*</sup>, Zulfiah<sup>2,b</sup>, Muh. Riswan Anas Sukri<sup>1,c</sup>, Yohanis T. Batlolona<sup>1,d</sup>, Wildan Nur Hamzah<sup>3,e</sup>**

<sup>1</sup> Department of Geophysical Engineering, Universitas Pattimura, Jl. Ir. M. Putuhena Kampus Poka, Ambon 97223, Indonesia

<sup>2</sup> Department of Geological Engineering, Universitas Pattimura, Jl. Ir. M. Putuhena Kampus Poka, Ambon 97223, Indonesia

<sup>3</sup> Departement of Earth Resource Sciences, Faculty of International Resource Sciences, Akita University, 1-1 Tegata gakuenmachi, Akita 010-8502, Japan

e-mail: <sup>a</sup>[samsul.bahri@fatek.unpatti.ac.id](mailto:samsul.bahri@fatek.unpatti.ac.id), <sup>b</sup>[zulfiah.zlfh@gmail.com](mailto:zulfiah.zlfh@gmail.com), <sup>c</sup>[muh.riswan.as@gmail.com](mailto:muh.riswan.as@gmail.com),  
<sup>d</sup>[yohanesbatlolona@gmail.com](mailto:yohanesbatlolona@gmail.com) and <sup>e</sup>[wildannurhamzah@gmail.com](mailto:wildannurhamzah@gmail.com)

\* Corresponding Author

---

Received: .....; Revised: .....; Accepted: .....

---

### Abstract

Identifying aquifer characteristics is vital for groundwater management, especially in volcanic terrains. This study employs Electrical Resistivity Tomography (ERT) combined with Archie's Law to delineate subsurface lithology and estimate aquifer porosity in Warasia, Ambon City. Field data were collected using a resistivity meter with two ERT profiles extending 120 meters each. The resistivity data were processed and modeled using RES2DINV, while water samples from wells were analyzed for physical parameters, including pH, conductivity, and total dissolved solids (TDS). The results reveal aquifers at depths of 3–5 meters, primarily hosted in volcanic tuff with resistivity values of 4.22–72.7  $\Omega\text{m}$ , indicating moderate to fair porosity (7.20%–14.01%). In contrast, lava formations exhibit significantly lower porosity (0.82%–1.02%) due to their solid structure. Archie's Law was instrumental in correlating resistivity with porosity, considering local lithological variability. The findings underscore the effectiveness of integrating ERT and Archie's Law for groundwater exploration in complex geological settings.

**Keywords:** Aquifer Characteristics, Electrical Resistivity Tomography (ERT), Archie's Law, Groundwater Porosity, Volcanic Lithology

**How to cite:** Bahri S, Zulfiah, Sukri MRA, Batlolona YT, Hamzah WN. The Manuscript Template of Jurnal Penelitian Fisika dan Aplikasinya (JPFA). *Jurnal Penelitian Fisika dan Aplikasinya (JPFA)*. 2025; 15(1): 27-39. DOI: <https://doi.org/10.26740/jpfa.v15n1.p27-39>.

---

© 2025 Jurnal Penelitian Fisika dan Aplikasinya (JPFA). This work is licensed under [CC BY-NC 4.0](https://creativecommons.org/licenses/by-nc/4.0/)

---

### INTRODUCTION

Groundwater is an essential and abundant freshwater resource, vital for sustaining human activities in the domestic and industrial sectors [1], [2]. The storage and mobility of groundwater are influenced by the porosity and permeability provided by pores and fractures in soil or rock. Groundwater movement is usually slow, ranging from 0.01 to 10 m/day [2], with residence times in storage ranging from tens to thousands of years [2], [3]. Groundwater resources can be controlled

by several factors, including topography, geological conditions, and vegetation [4], [5], [6]. Identifying the aquifer and understanding the groundwater system provides valuable insight into exploration plans and developments.

Electrical resistivity tomography (ERT) is a non-invasive and low-cost geophysical method commonly used to interpret and identify the aquifer zone [7], [8]. Groundwater identification through ERT is a well-established method that leverages the relationship between electrical resistivity and porosity, as described by Archie's Law. This empirical relationship is crucial for estimating aquifer porosity, particularly in saturated, non-clay media. Archie's Law states that the bulk resistivity of a saturated rock is related to the resistivity of the pore water and the rock's porosity, allowing porosity to be calculated from resistivity measurements [9], [10]. The application of Archie's Law in ERT involves measuring the electrical resistivity of subsurface materials, which can be influenced by factors such as pore-space saturation and rock mineral composition. For instance, studies have shown that resistivity and porosity data can be modeled effectively using Archie's Law, even in complex geological settings such as fault zones, where variations in microstructure and mineralogy occur [11]. This adaptability of Archie's Law underscores its utility in diverse geological contexts, including volcanic deposits and carbonate reservoirs, where deviations from the classic model can occur due to heterogeneity [12].

Moreover, integrating ERT with other geophysical methods enhances the accuracy of porosity estimates. For example, combining electrical resistivity data with seismic measurements has been proposed as a method to evaluate both porosity and degree of saturation effectively [13]. This multi-faceted approach can mitigate issues arising from lithological heterogeneity and improve the reliability of groundwater assessments in complex environments [14]. In practical applications, the parameters derived from Archie's Law, such as the cementation factor ( $m$ ) and the saturation exponent ( $n$ ), are critical for accurately interpreting resistivity data. These parameters can vary significantly depending on the geological context and the physical properties of the materials involved [15]. For instance, research indicates that the cementation exponent is not universally applicable across different reservoirs, suggesting that localized calibration may be necessary to achieve reliable results.

Furthermore, recent technological advancements, such as high-resolution imaging techniques and pore-network modeling, have provided more profound insights into the electrical transport properties of porous media, enabling a more nuanced application of Archie's Law [16], [17]. The research location is in Warasia Village, Ambon City. This area is situated in a hilly region with a lithology predominantly composed of volcanic rock. The majority of the population utilizes surface water from the river, while some use dug wells to meet their daily needs. Groundwater use is highly recommended for this area due to its more stable quality and quantity compared to surface water sources or dug wells. These innovations facilitate a better understanding of how pore connectivity and morphology influence resistivity measurements, which is essential for accurate groundwater identification and management. This study aims to identify the characteristics of the aquifer system using ERT data and calculations based on Archie's Law. Measurement of water's physical parameters, such as pH, salinity, TDS, and electrical conductivity, is needed to calculate rock formation porosity.

## MATERIALS AND METHOD

### Geology of Study Area

Warasia is one of the sub-villages in Batu Merah Village, Sirimau District, Ambon City. The lithology of Ambon is dominated by Ambon volcanic rocks (Ambonites), coral limestone, and sedimentary deposits (See Fig. 1). Ambonites, primarily composed of cordierite- and garnet-bearing dacites, are indicative of the volcanic activity that has shaped the island's geological landscape. These rocks are believed to be the volcanic equivalent of cordierite granites found in the area, suggesting a significant relationship between volcanic and granitic processes in the formation of the island's lithology [10]. In addition to volcanic lithology, Ambon's geological composition includes a variety of sedimentary rocks and alluvial deposits, which are essential for understanding the island's broader geological framework. The Late Pliocene to Holocene lithology of Ambon encompasses not only volcanic rocks and reef limestone but also alluvial sediments, indicating a diverse geological history influenced by both marine and terrestrial processes [18], [19].

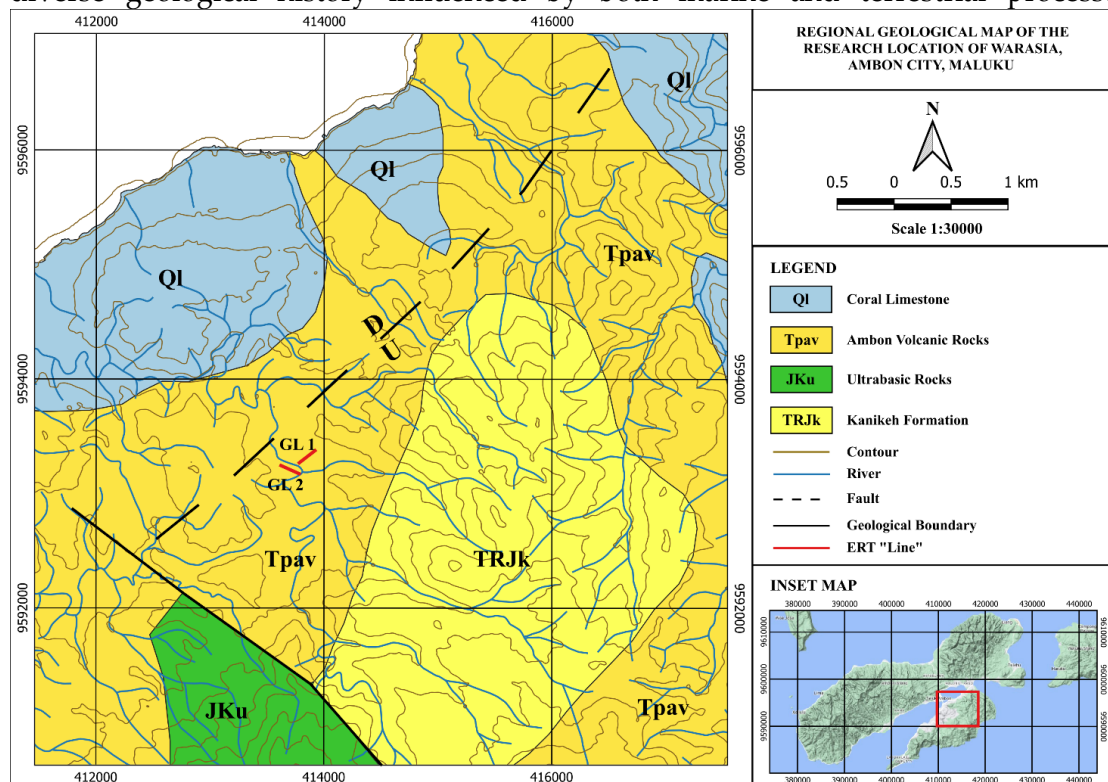


**Figure 1.** Regional geological map of the Warasia area, Ambon City, consisting of coral limestone, Ambon volcanic rocks, ultrabasic rocks, Kanikeh formation.

Our research site is located in an area of Ambon affected by volcanic activity. One of the main products of this formation is volcanic breccia, formed by explosive eruptions and then deposited. In the vicinity of the study site, there are outcrops of volcanic breccia that can be observed on the banks of the river, as shown in Fig. 2. At the time of field observation, the volcanic breccia found in the research location area is a volcanic breccia with a brown color, consisting of fragments and matrix. The fragment has coarse lapilli, blocking the grain size, and the matrix is fine-grained tuff. The fragment is basaltic, dark gray in color, aphanitic in texture, and contains pyroxene, plagioclase, biotite, and volcanic glass.



**Figure 2.** (a) Volcanic breccia and tuff outcrops found near the ERT line, (b) Close up view of tuff

### ERT Data Collection

The electrical resistivity method is a widely utilized geophysical technique that measures the electrical resistivity of subsurface materials to infer geological structures and properties. This method is particularly advantageous for hydrogeological studies, as it enables delineation and characterization of groundwater aquifers. The resistivity values obtained can be correlated with hydrogeological properties such as porosity and permeability, providing insights into the subsurface water resources [20], [21]. The method's popularity stems from its cost-effectiveness, ease of operation, and ability to cover large areas, making it a preferred choice over conventional geotechnical testing methods.

The electrical resistivity method typically employs various electrode configurations, with the Wenner method among the most common. In this configuration, a direct current (DC) is applied through outer electrodes, while the potential difference is measured across inner electrodes. The resistivity is calculated using the geometric factor associated with the electrode arrangement, which is crucial for accurate interpretation of the subsurface conditions [22], [23], [24]. This technique can be implemented in both 2D and 3D imaging formats, enabling detailed mapping of subsurface features and the identification of geological anomalies, such as sinkholes and cavities [25], [26]. In practical applications, the electrical resistivity method has been employed in various fields, including environmental monitoring, archaeological investigations, and geotechnical engineering [27].

### Archie's Law

Archie's law is a fundamental empirical relationship in petrophysics that connects the electrical resistivity of saturated porous media to porosity and fluid saturation [28]. The general equation for Archie's law is given in equation 1. Where  $\rho_t$  is the resistivity of the rock formation,  $\rho_w$  is the resistivity of the formation water,  $a$  is the tortuosity,  $\phi$  is the porosity of the rock,  $S_w$  is the cementation factor,  $n$  is the saturation of the formation water, and  $n$  is the saturation exponent.

$$\rho_t = \rho_w \cdot a \cdot \phi^{-m} \cdot S_w^n \quad (1)$$

The empirical nature of Archie's law has been substantiated by numerous studies demonstrating its applicability across diverse geological formations. For instance, Hamahashi et al. highlighted that the relationship between porosity and resistivity in fault zones is well described by Archie's

law, with specific values for the cementation exponent [11]. Similarly, Cai et al. confirmed the validity of Archie's equation for modeling electrical conductivity in fractal porous media, suggesting that the law holds under specific porosity and saturation conditions [29].

Archie's law has also been examined in the context of percolation theory, which provides a theoretical underpinning for the observed relationships in porous media. Hunt discussed how the law arises from percolation scaling, particularly in systems where the percolation critical volume fraction is proportional to the porosity (Hunt, 2004). This theoretical framework is essential for understanding the limitations and applicability of Archie's law, especially in heterogeneous materials like carbonates, where the parameters can vary significantly [30]. The parameters  $m$  and  $n$  are critical for accurately applying Archie's law. In many water-wet formations, these exponents are typically close to 2, as noted by Montaron [31]. However, variations in rock texture and pore structure can lead to deviations from this norm, necessitating careful calibration of the parameters for specific formations. The constant values  $a$  and  $m$  for Archie's law across several lithologies are shown in Table 1.

**Table 1.** The constant values  $a$  and  $m$  for use in Archie's law for several types of lithology [32].

Rock Description	$a$	$m$
weakly cemented clastic rocks, such as sand, sandstone and some limestones (Tertiary age)	0.88	1.37
Moderately well cemented sedimentary rocks, including sandstone and limestone (Mesozoic age)	0.62	1.72
well-cemented sedimentary rock (Paleozoic age)	0.62	1.95
Highly porous volcanic rocks, such as tuff, and Pahoehoe	3.5	1.44
solid igneous rock and metamorphic sedimentary rock	1.4	1.58

In practical applications, Archie's law serves as a vital tool in hydrocarbon exploration and reservoir characterization. It allows geoscientists to estimate hydrocarbon saturation from resistivity measurements, which is crucial for resource evaluation [28], [33]. However, the law's assumptions, particularly regarding the uniformity of pore space and fluid distribution, can lead to inaccuracies in certain geological contexts, such as in the presence of complex pore networks or varying fluid saturations [8], [27].

## RESULTS AND DISCUSSION

### ERT Results and Lithological Interpretation

ERT measurements were conducted on August 29, 2024, on two tracks in the Warasia area, Ambon City. Both tracks are 120 meters long and have an estimated depth of around 18 meters. Measurements were made using the Naniura Resistivitymeter NRD 300 Plus tool with an additional 40 Channel switch box. The measurement results are the electric current and voltage responses; from these two data, the apparent resistivity will be obtained using the Henkel transformation. The distribution of subsurface resistivity is obtained from inversion modeling using RES2DINV. Line 1 runs in a SW-NE direction, with the midpoint at coordinates 030°40'45.60" LS and 1280°13'26.37" BT. At the same time, the second line of ERT has an SE-NW direction with the midpoint at coordinates 3°40'47.86" LS and 128°13'24.79" BT. The ERT line map is shown in Fig.

3. Both tracks are in a valley near a river, with topography ranging from 64 to 68 meters above sea level. In the research area, there are five wells with groundwater depths of 3-5 meters.

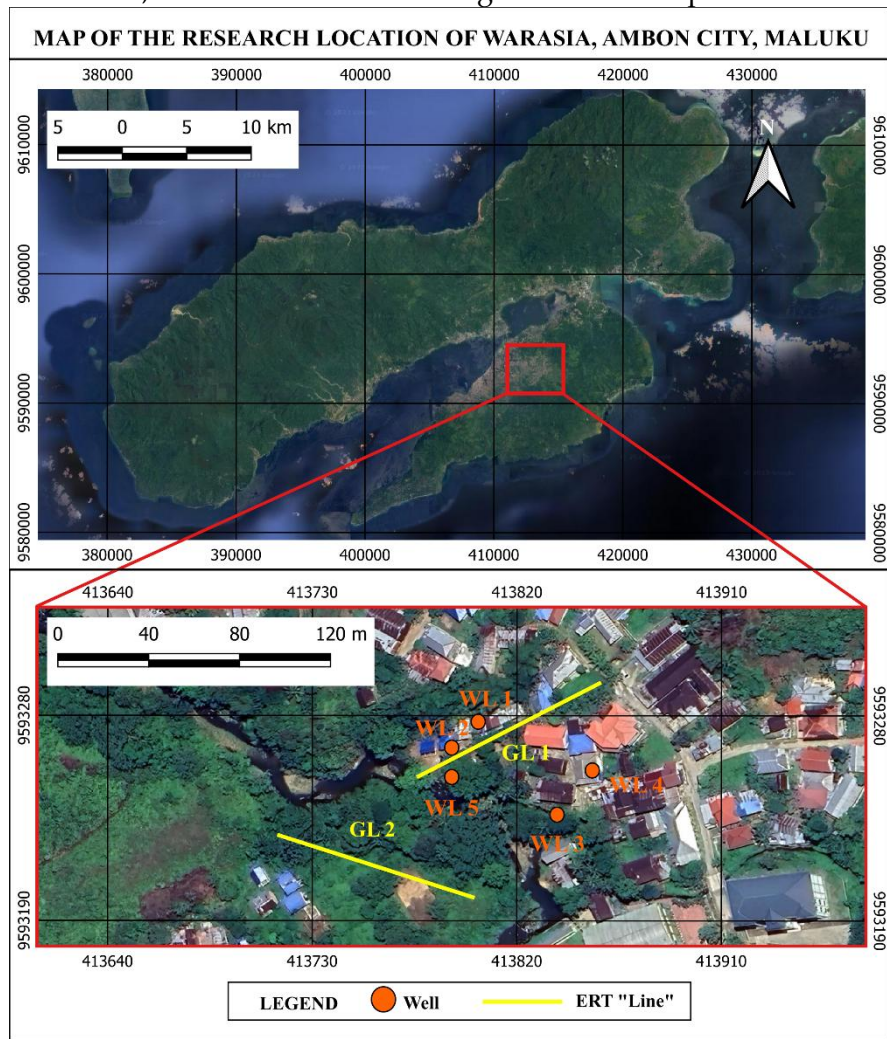


**Figure 3.** Line of ERT Map and Location of Dug Well Points in the Research Area

In GL 1, the resistivity value range obtained is  $4.22 - 423.31 \Omega\text{m}$ , as shown in Fig. 4(a). This line has a perpendicular direction to the river flow. The conductive zone was found in the second layer at a depth of about 3 meters which is marked with blue to yellow ( $4.22 - 72.7 \Omega\text{m}$ ). This layer is suspected to be an aquifer in the form of water-saturated tuff. This result is also supported by observations of the depth of the groundwater level in the dug well near the electrical resistivity measurement which has a similar depth. While the layer above it is more resistive with a resistivity value of more than  $72.7 \Omega\text{m}$  and is interpreted as volcanic breccia. This interpretation is based on observations of the outcrops in Fig. 2. At a depth of 12 meters there is a resistive layer which is suspected to be lava or ambonite. The interpretation of lithology on line 1 can be seen in Fig. 4(b).

The results obtained are similar to the interpretation of electrical resistivity measurements in other volcanic areas, such as the Lam Apeng area in Aceh Besar, Indonesia, which is part of the Lam Teuba Volcanics formation. Based on the ERT results, the subsurface conditions are divided into three layers, with the aquifer in the second layer, which has a low resistivity ( $12 - 18.6 \Omega\text{m}$ ) at

a depth of 8 - 18 metres. The aquifer layer is flanked by a high resistivity layer interpreted as pyroclastic deposits at the surface and tuff in the third layer [34]. Similar research in Solok, West Sumatra, also shows that groundwater is expected to be in the low-resistivity layer (< 26.2  $\Omega$ m). At the same time, layers with high resistivity are interpreted as Basalt, Andesite, or Lava [35]. These types of rocks tend to be massive and lack voids, making it difficult to store and pass water [36]. GL 2 has a trajectory direction parallel to the river flow. The range of resistivity values obtained from the inversion modeling results on this trajectory is 10.93 - 3,869.40  $\Omega$ m, as shown in Figure 5(a). Almost identical to trajectory 1, this trajectory indicates that the conductive zone began at a depth of 2.5 meters and is likely an aquifer layer. The upper layer is a pyroclastic deposit in the form of volcanic breccia, which is more resistant. In this layer, lava flows were found with resistivities exceeding 400  $\Omega$ m. Lava rocks of cordierite dacite are found in several areas of Ambon, including Hitu [37]. The presence of cordierite in these dacite rocks indicates high-temperature conditions during their formation, indicating significant magmatic influence and potential crustal anatexis [38]. This type of rock is generally solid and has poor porosity. The results of the lithology interpretation for line 2 are shown in Figure 5(b).

The GL2 line (40-60 m, Figure 5) displays a vertical discontinuity with a 60° northwest dip, highlighted by shifts in low- and high-resistivity values. This discontinuity is interpreted as a structural boundary and aligns with the dip-slip fault identified by Cokrosapoetro et al. (1993). Comparable fault interpretations using electrical resistivity imaging, as reported by Kuria et al. (2010) and Seminsky et al. (2016) [39], correlate vertically low-resistivity boundaries with fault zones characterized by greater fracture intensity, enhanced porosity, and permeability. This study aims to identify prospective aquifer zones and delineate low resistivity distributions suggestive of aquifers. Further fault-mapping analysis is necessary to confirm the fault's existence.

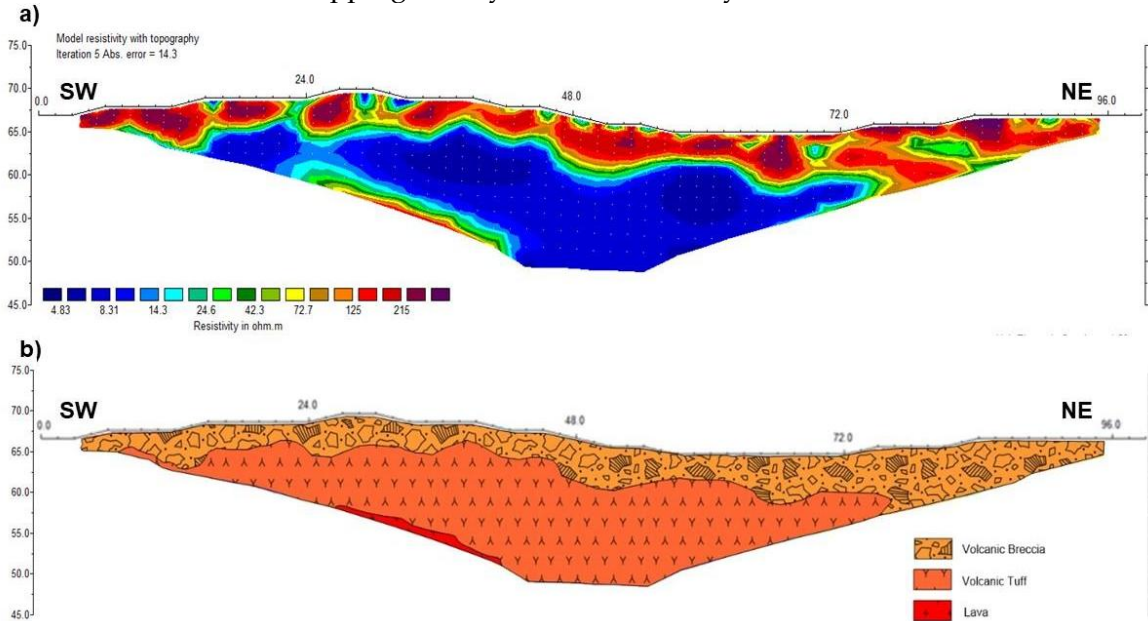


**Figure 4.** (a) Distribution of subsurface resistivity from inversion modeling, and (b) interpretation of lithology in GL 1

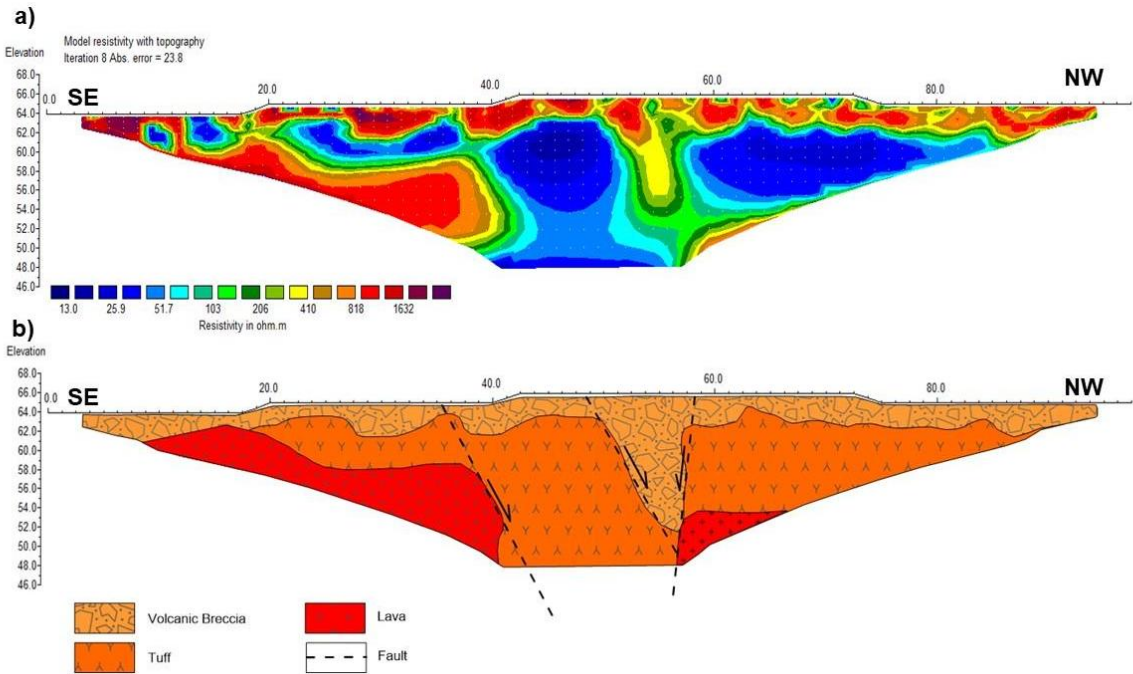


**Figure 5.** (a) Distribution of subsurface resistivity from inversion modeling, and (b) interpretation of lithology in GL 2.

### The Analysis of Rock's Porosity and Aquifer Characteristics

Rock porosity is one of the main factors that affect the quality and quantity of fluid in an aquifer. Porosity refers to the amount of empty space or pores in a rock that allows fluid to flow or be stored. Calculation of rock porosity values using Archie's Law which connects the value of rock resistivity, formation water resistivity, and porosity. Measurement of the physical properties of water was carried out on 5 water samples taken from 4 wells and in river water. The parameters of the physical properties of water measured include pH, electrical conductivity, Total Dissolved Solid (TDS), and salinity. The measurement results can be seen in Table 2.

**Table 2.** Results of Physical Water Parameter Measurements at Several Dug Well Point Locations

No. Sample	pH	Conductivity ( $\mu\text{S}/\text{cm}$ )	TDS (ppm)	Salinity (%)	Resistivity ( $\Omega\text{m}$ )
WL-1	6.60	191	95	0.00	52.35
WL-2	6.46	134	68	0.00	74.63
WL-3	5.22	206	103	0.00	48.54
WL-4	5.34	220	111	0.00	45.45
WL-5	6.76	212	104	0.00	47.17
<b>Average</b>	<b>6.08</b>	<b>192.6</b>	<b>96.2</b>	<b>0.00</b>	<b>53.63</b>

Based on the data in table 2, the average value of the acidity level in groundwater in the Warasia area is 6.08. The TDS values show a positive correlation with conductivity and a negative correlation with resistivity. TDS describes the amount of dissolved solids in water, which mostly consist of ions. An increase in the number of ions will simultaneously increase electrical conductivity [30]. TDS and conductivity values can be used as a reference to determine the *Bahri et al*

suitability of water for consumption, where water is considered good for consumption if the TDS value is <500 ppm and Conductivity <500  $\mu\text{S}/\text{cm}$ . So based on these data in this area, groundwater is classified as good for consumption. The resistivity of formation water can be obtained from the conductivity value, where resistivity is the inverse of conductivity.

By utilizing the equation in Archie's law we can predict the porosity of rocks below the surface. Based on the subsurface interpretation of ERT data, it is found that the water-saturated rocks are Tuff and Lava. Tuff has a lower resistivity value and generally tends to be more porous compared to more solid lava. Because both types of lithology are below the water table, they are saturated with water and the formation water saturation value approaches 1 ( $S_w = 1$ ). Based on equation (1) we get the rock porosity value on both tracks as shown in Table 3.

**Table 3.** Rock Porosity Values in the Research Area Based on Calculations Using Archie's Law

Line of ERT	Lithology	Porosity (%)	Quality
GL-1	Volcanic Tuff	14.01	Fair
	Lava	1.02	Negligible
GL-2	Volcanic Tuff	7.20	Poor
	Lava	0.82	Negligible

On the GL-2 line, there tends to be a higher distribution of subsurface resistivity values compared to the GL-1 line. This is associated with rock type, porosity, and water saturation level. Based on the calculation results shown in Table 3, the volcanic tuff lithology has porosity values of 7.20% - 14.01%, while lava has porosity values of 0.82% - 1.02%. The quality of volcanic tuff porosity in this area is classified as poor to moderate, while the lava lithology is very poor. Volcanic tuff, formed from the consolidation of volcanic ash, exhibits varying porosity influenced by its mineral composition, depositional environment, and diagenetic processes. In addition, lithofacies and mineral composition also affect the porosity value of tuff rocks. Research shows that tuffaceous mudstone, sedimentary tuff, and other tuff types have average porosities of 6.5%, 5.09%, and 3.86%, respectively, highlighting the variability in porosity across tuff types [40]. In contrast, volcanic lavas typically have lower porosity than tuffs, mainly because they have a denser, more crystalline structure. Tuffs are often formed during explosive volcanic events, leading to a more fragmented, porous structure, while lava flows are usually associated with effusive eruptions, resulting in denser formations. Nilai porositas

The determination of porosity value using Archie's Law in this study still uses secondary data related to the tortuosity value (a) and cementation factor (m). To increase accuracy, boreholes can be drilled to obtain rock samples below the surface, and testing can be performed to obtain physical data on the rock. The use of other methods, such as refraction, seismic, or Audio Magnetotelluric (ADMT), can also be added to increase interpretation accuracy. The integration of ERT and Archie's Law can help characterize aquifers in an area and select the point and type of borehole for groundwater exploration.

## CONCLUSION

Based on the research results in the Warasia area, groundwater is at a depth of about 4 meters, where the water-bearing rock is volcanic tuff with a resistivity value of 4.22 -72.7  $\Omega\text{m}$ . Groundwater in this area is abundant and evenly distributed. The aquifers in this area are shallow and are

strongly influenced by surface water. The overburden layer consists of volcanic breccia pyroclastic rocks with resistivity ranging from 72.7 to 400  $\Omega$ m. In this area, lava flows with resistivity > 400  $\Omega$ m were also found. Based on measurements of water physical property parameters and ERT data, we can estimate rock porosity using Archie's Law. The volcanic tuff lithology has poor to moderate porosity (7.20% - 14.01%), while lava has very poor porosity (0.82% - 1.02%).

## AUTHOR CONTRIBUTIONS

Samsul Bahri: Conceptualization, Methodology, Writing - Original Draft, and Writing - Review & Editing; Zulfiah: Methodology, Formal Analysis, Validation; Muh. Riswan Anas Sukri: Data Curation, Project Administration, and Writing - Review & Editing; Yohanis T. Batlolona: Data Curation, Project administration, and Software; and Wildan Nur Hamzah: Writing – Review, Validation and Data Curation.

## DECLARATION OF COMPETING INTEREST

The authors declare that they have no known competing financial interests or personal relationships that could have appeared to influence the work reported in this paper.

## REFERENCES

- [1] S. Siebert *et al.*, "Groundwater use for irrigation - A global inventory," *Hydrol. Earth Syst. Sci.*, vol. 14, no. 10, pp. 1863–1880, 2010, doi: <https://doi.org/10.5194/hess-14-1863-2010>.
- [2] M. Velis, K. I. Conti, and F. Biermann, "Groundwater and human development: synergies and trade-offs within the context of the sustainable development goals," *Sustain. Sci.*, vol. 12, no. 6, pp. 1007–1017, 2017, doi: <https://doi.org/10.1007/s11625-017-0490-9>.
- [3] S. Foster, J. Chilton, G. J. Nijsten, and A. Richts, "Groundwater-a global focus on the 'local resource,'" *Curr. Opin. Environ. Sustain.*, vol. 5, no. 6, pp. 685–695, 2013, doi: <https://doi.org/10.1016/j.cosust.2013.10.010>.
- [4] X. Zhang, J. J. Jiao, and W. Guo, "How Does Topography Control Topography-Driven Groundwater Flow?," *Geophys. Res. Lett.*, vol. 49, no. 20, 2022, doi: <https://doi.org/10.1029/2022GL101005>.
- [5] X. Chen *et al.*, "Study on the Impact of Vegetation Restoration on Groundwater Resources in Tianshan Mountain and Yili Valley in Xinjiang, China," *Water (Switzerland)*, vol. 16, no. 5, 2024, doi: <https://doi.org/10.3390/w16050696>.
- [6] X. Kuang *et al.*, "The changing nature of groundwater in the global water cycle," *Science (80. ).*, vol. 383, no. 6686, 2024, doi: <https://doi.org/10.1126/science.adf0630>.
- [7] H. M. El-Sayed and A. R. Elgendi, "Geospatial and geophysical insights for groundwater potential zones mapping and aquifer evaluation at Wadi Abu Marzouk in El-Nagila, Egypt," *Egypt. J. Aquat. Res.*, vol. 50, no. 1, pp. 23–35, 2024, doi: <https://doi.org/10.1016/j.ejar.2023.12.008>.
- [8] T. Takele, M. Husein, D. Diriba, and G. Assefa, "Application of electrical resistivity tomography for groundwater evaluation in Yirgacheffe Town and its environs, Main Ethiopian Rift," *HydroResearch*, vol. 8, pp. 202–208, 2025, doi: <https://doi.org/10.1016/j.hydres.2024.11.003>.
- [9] N. Somaratne, "Karst Conduit Networks , Connectivity and Recharge Dynamics of a Sinkhole," *Environ. Nat. Resour. Res.*, vol. 7, no. 3, pp. 70–88, 2017, doi: <https://doi.org/10.1016/j.hydres.2024.11.003>.

- [10] F. R. Carneiro, A. A. Neto, R. M. R. de Almeida, and S. de Matos Mello, "Geotechnical description of sandy sediments of the surf zone using electrical resistivity measurements," *Rev. Bras. Geofis.*, vol. 36, no. 3, pp. 283–296, 2018, doi: <https://doi.org/10.22564/RBGF.V36I3.1952>.
- [11] M. Hamahashi *et al.*, "Contrasts in physical properties between the hanging wall and footwall of an exhumed seismogenic megasplay fault in a subduction zone – An example from the Nobeoka Thrust Drilling Project," *Geochemistry Geophys. Geosystems*, vol. 14, no. 12, pp. 5354–5370, 2013, doi: <https://doi.org/10.1002/2013GC004818>.
- [12] D. Z. Mutaqin, A. D. Haryanto, and U. Mardiana, "Contribution of Resistivity Properties in Estimating Hydraulic Conductivity in Ciremai Volcanic Deposits," *Jambura Geosci. Rev.*, vol. 5, no. 1, pp. 51–62, 2023, doi: <https://doi.org/10.34312/jgeosrev.v5i1.17333>.
- [13] R. . Cosentini and S. Foti, "Evaluation of porosity and degree of saturation from seismic and electrical data," *Geotechnique*, vol. 64, no. 4, pp. 278–286, 2014, doi: <https://doi.org/10.1680/geot.13.P.075>.
- [14] M. J. Stephens, D. H. Shimabukuro, J. M. Gillespie, and W. Chang, "Groundwater salinity mapping using geophysical log analysis within the Fruitvale and Rosedale Ranch oil fields , Kern County ,," *Hydrogeol. J.*, vol. 27, pp. 731–746, 2018, doi: <https://doi.org/10.1007/s10040-018-1872-5>.
- [15] H. Dashtian, Y. Yang, and M. Sahimi, "Nonuniversality of the Archie exponent due to multifractality of resistivity well logs," *Geophys. Res. Lett.*, vol. 42, no. 10, pp. 655–662, 2015, doi: <https://doi.org/10.1002/2015GL066400>.
- [16] D. Bauer *et al.*, "From computed microtomography images to resistivity index calculations of heterogeneous carbonates using a dual-porosity pore-network approach: Influence of percolation on the electrical transport properties," *Phys. Rev. E - Stat. Nonlinear, Soft Matter Phys.*, vol. 84, no. 1, pp. 1–12, 2011, doi: <https://doi.org/10.1103/PhysRevE.84.011133>.
- [17] J. Zhao *et al.*, "Pore-Scale Investigation of the Electrical Property and Saturation Exponent of Archie ' s Law in Hydrate-Bearing Sediments," *J. Mar. Sci. Eng.*, vol. 10, no. 111, 2022, doi: <https://doi.org/10.3390/jmse10010111>.
- [18] S. Bahri, A. Ramadhan, and Zulfiah, "Investigation of Groundwater Quality using Vertical Electrical Sounding and Dar Zarrouk Parameter in Leihitu, Maluku, Indonesia," *J. Geosci. Eng. Environ. Technol.*, vol. 8, no. 3, pp. 221–228, 2023, doi: <https://doi.org/10.25299/jgeet.2023.8.3.12976>.
- [19] R. Lewerissa, S. Sismanto, A. Setiawan, and S. Pramumijoyo, "The igneous rock intrusion beneath ambon and seram islands, eastern Indonesia, based on the integration of gravity and magnetic inversion: Its implications for geothermal energy resources," *Turkish J. Earth Sci.*, vol. 29, no. 4, pp. 596–616, 2020, doi: <https://doi.org/10.3906/yer-1908-17>.
- [20] M. A. A. Mohammed, N. P. Szabó, and P. Szűcs, "Delineation of groundwater potential zones in northern Omdurman area using electrical resistivity method Delineation of groundwater potential zones in northern Omdurman area using electrical resistivity method," *IOP Conf. Ser. Earth Environ. Sci.*, vol. 1189, no. 012012, 2023, doi: <https://doi.org/10.1088/1755-1315/1189/1/012012>.
- [21] V. Wayal, T. G. Sitharam, and G. M. Latha, "Geo-electrical Evaluation of Compacted Sand-Bentonite Mix Characteristics," in *6th World Congress on Civil, Structural, and Environmental*

- [22] A. S. Dias, V. Gingine, and R. Cardoso, "Correspondence between electrical resistivity and total suction in compacted kaolin considering the presence of salt," in *E3S Web of Conferences*, 2016, p. 10002. doi: <https://doi.org/10.1051/e3sconf/20160910002>.
- [23] C. Masciopinto, I. S. Liso, M. C. Caputo, and L. De Carlo, "An Integrated Approach Based on Numerical Modelling and Geophysical Survey to Map Groundwater Salinity in Fractured Coastal Aquifers," *water*, vol. 9, no. 875, pp. 1–13, 2017, doi: <https://doi.org/10.3390/w9110875>.
- [24] S. Bahri, S. V. Aponno, and Zulfiah, "Global Optimization Very Fast Simulated Annealing Inversion For The Interpretation of Groundwater Potential," *J. Geofis. Eksplor.*, vol. 08, no. 03, pp. 225–236, 2022, doi: <https://doi.org/10.23960/jge.v8i3.233>.
- [25] H. H. Karim, M. R. Al-Qaissy, and N. A. Aziz, "Differentiating Clayey Soil Layers from Electrical Resistivity Imaging (ERI) and Induced Polarization (IP)," *Eng. Tech. J.*, vol. 31, no. 17, pp. 2316–2334, 2013, doi: <https://doi.org/10.30684/etj.31.17a.1>.
- [26] M. Grigorova and I. Koprev, "3D Model of Limestone Inclusions in Maritsa Iztok Mine Based on Electrical Resistivitas Tomography," *Acta Geobalcanica*, vol. 3, no. 2, pp. 51–56, 2017, doi: <https://doi.org/10.18509/AGB.2017.06>.
- [27] S. Bahri, D. Tualepe, Y. T. Batlolona, A. Ramadhan, and W. W. Parnadi, "Vertical electrical sounding method and Dar Zarrouk analysis to identify the distribution of seawater intrusion in Pelauw Village, Maluku," *J. Degrad. Min. Lands Manag.*, vol. 11, no. 4, pp. 6089–6097, 2024, doi: <https://doi.org/10.15243/jdmlm.2024.114.6089>.
- [28] P. W. J. Glover, "Archie's law - A reappraisal," *Solid Earth*, vol. 7, no. 4, pp. 1157–1169, 2016, doi: <https://doi.org/10.5194/se-7-1157-2016>.
- [29] W. Wei, J. Cai, X. Hu, and Q. Han, "An electrical conductivity model for fractal porous media," *Geophys. Res. Lett.*, vol. 42, no. 12, pp. 4833–4840, 2015, doi: <https://doi.org/10.1002/2015GL064460>.
- [30] G. M. Hamada, A. A. Almajed, T. M. Okasha, and A. A. Albathe, "Uncertainty analysis of Archie's parameters determination techniques in carbonate reservoirs," *J. Pet. Explor. Prod. Technol.*, vol. 3, no. 1, pp. 1–10, 2013, doi: <https://doi.org/10.1007/s13202-012-0042-x>.
- [31] B. Montaron, "A Quantitative Model for the Effect of Wettability on the Conductivity of Porous Rocks," 2007, doi: <https://doi.org/10.2523/105041-ms>.
- [32] G. V Keller, "Rock and Mineral Properties," in *Electromagnetic methods in applied geophysics*, 1987, pp. 13–52, doi: <https://doi.org/10.1190/1.9781560802631.ch2>.
- [33] K. Li, B. Pan, and R. Horne, "Evaluating fractures in rocks from geothermal reservoirs using resistivity at different frequencies," *Energy*, vol. 93, pp. 1230–1238, 2015, doi: <https://doi.org/10.1016/j.energy.2015.09.084>.
- [34] D. Darisma, F. Fernanda, and M. Syukri, "Investigation of Groundwater Potential using Electrical Resistivity Method and Hydraulic Parameters in Lam Apeng, Aceh Besar, Indonesia," *J. Geosci. Eng. Environ. Technol.*, vol. 5, no. 4, pp. 185–190, 2020, doi: <https://doi.org/10.25299/jgeet.2020.5.4.5501>.
- [35] E. Ariani and Akmam, "Mapping of rock resistivity value using geoelectrical method Schlumberger configuration in Solok Regency, West Sumatera," *J. Phys. Theor. Appl.*, vol. 3, no. 1, pp. 27–35, 2019, doi: <https://doi.org/10.20961/jphystheor-appl.v3i1.38134>.
- [36] V. Navelot *et al.*, "Petrophysical Properties of Volcanic Rocks and Impacts of Hydrothermal

Alteration in the Guadeloupe Archipelago (West Indies)," *J. Volcanol. Geotherm. Res.*, vol. 360, pp. 1–21, 2018, doi: <https://doi.org/10.1016/j.jvolgeores.2018.07.004>.

- [37] S. Sismanto and R. Lewerissa, "Analytic Signal and Reservoir Model of Hatuasa-Talanghaha Hot Spring, Tulehu, Ambon, Indonesia Based on Magnetic Data Inversion," *Int. J. Civ. Eng. Technol.*, vol. 11, no. 1, pp. 137–145, 2020, doi: <https://doi.org/10.34218/ijciet.11.1.2020.015>.
- [38] J. M. Pownall, M. A. Forster, R. Hall, and I. M. Watkinson, "Tectonometamorphic evolution of Seram and Ambon, eastern Indonesia: Insights from  $^{40}\text{Ar}/^{39}\text{Ar}$  geochronology," *Gondwana Res.*, vol. 44, no. April, pp. 35–53, 2016, doi: <https://doi.org/10.1016/j.gr.2016.10.018>.
- [39] K. Z. Seminsky, R. M. Zaripov, and V. V. Olenchenko, "Interpretation of shallow electrical resistivity images of faults: tectonophysical approach," *Russ. Geol. Geophys.*, vol. 57, no. 9, pp. 1349–1358, 2016, doi: <https://doi.org/10.1016/j.rgg.2016.08.020>.
- [40] R. Li, Z. Xiong, Z. Wang, W. Xie, W. Li, and N. Su, "characteristics of Permian marine tuffaceous rocks in the Sichuan Basin," *Front. Earth Sci.*, vol. 10, no. 1054276, pp. 1–18, 2023, doi: <https://doi.org/10.3389/feart.2022.1054276>.